

$\omega \rightarrow \pi\pi$ decay in nuclear medium[★]

Wojciech Broniowski^a, Wojciech Florkowski^a, and
Brigitte Hiller^b

^a*H. Niewodniczański Institute of Nuclear Physics, PL-31342 Kraków, Poland*

^b*Center for Theoretical Physics, University of Coimbra, P-3000 Coimbra, Portugal*

Abstract

We calculate the width for the $\omega \rightarrow \pi\pi$ decay in nuclear medium. Chiral dynamics and low-density approximation are used. At densities around twice the nuclear saturation density we estimate the partial width for the decay of the longitudinal mode to be of the order of a few tens of MeV, and for the transverse mode a few times less.

Key words: relativistic heavy-ion collisions, vector mesons, in-medium modifications of particle properties

PACS: 25.75.Dw, 21.65.+f, 14.40.-n

Recent relativistic heavy-ion experiments have brought evidence that nuclear medium modifies substantially properties of meson excitations. In particular, the dilepton measurements in the CERES [1] and HELIOS [2] experiments indicate that either the positions of light vector mesons are shifted down or their widths are increased. Such a behavior is expected from many theoretical calculations [3–11] (for review see [12,13]). Among the sources of the in-medium modifications of meson properties are phenomena forbidden in the vacuum, which become possible in the presence of nuclear medium. In particular, constraints such as G -parity are no longer effective for mesons moving with respect to nucleons in nuclear matter.

In this Letter we analyze an example of such an “exotic” process: the in-medium decay of $\omega \rightarrow \pi\pi$.¹ This process has been recently analyzed by Wolf, Friman, and Soyeur

[★] Research supported by PRAXIS grants XXI/BCC/429/94 and PCEX/P/FIS/13/96, and by the Polish State Committee for Scientific Research grant 2P03B-080-12.

^{**}E-mail: broniows@solaris.ifj.edu.pl, florkows@solaris.ifj.edu.pl, brigitte@fteor5.fis.us.pt

¹ In the vacuum the process $\omega \rightarrow \pi^+\pi^-$ occurs with a 2% branching ratio. This is due to small isospin breaking and the resulting $\rho - \omega$ mixing. This is not the process we are concerned in this paper, hence we work in the strict isospin limit.

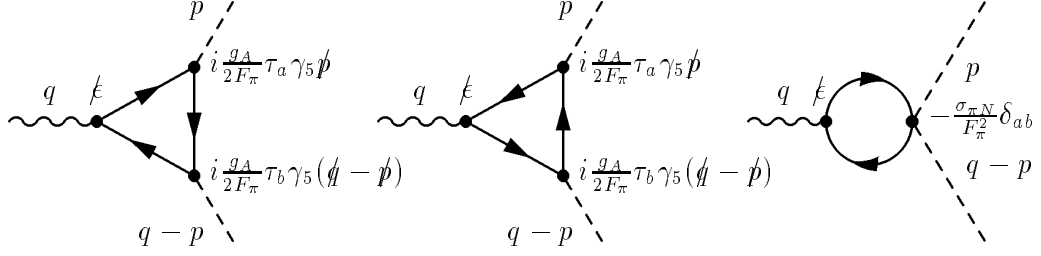


Fig. 1. One-nucleon-loop diagrams contributing to the $\omega \rightarrow \pi\pi$ amplitude in nuclear medium. Pseudovector coupling is used. The incoming ω has momentum q and polarization ϵ . The outgoing pions have momenta p and $q - p$, and isospin a and b , respectively. Pseudovector coupling is used in the first two diagrams. The third diagram contains the S-wave π - N coupling, proportional to the sigma term, $\sigma_{\pi N}$. The in-medium nucleon propagator is given in Eq. (1).

[14], where the $\omega - \sigma$ mixing mechanism and the subsequent decay of the σ into two pions leads to a huge partial decay width for $\omega \rightarrow \pi\pi$, of the order of a few hundred MeV at typical densities in relativistic heavy-ion collisions, and for ω moving with the momentum of the order of 500 MeV with respect to nuclear matter. We carefully reanalyze the calculation of Ref. [14]. Firstly, we recognize that at the same level of calculation (low-density expansion) there are additional diagrams in nuclear medium, leading to $\omega \rightarrow \pi\pi$ without an intermediate σ state (the first two diagrams in Fig. 2). The inclusion of these diagrams provides cancellations with the diagram with the intermediate σ state (third diagram in Fig. 2), which are strong when the mass of the σ is large. This can lead to a reduction of the in-medium partial width for $\omega \rightarrow \pi\pi$ down to a level of a few tens of MeV, which is much smaller than the value of Ref. [14], but still large enough to be relevant among other processes contributing to the in-medium ω width. More importantly, the inclusion of all diagrams in Fig. 2 is necessary to satisfy the constraints of chiral symmetry in formal limiting cases (small external 4-momenta). Also, we take the effort to analyze separately the longitudinally and transversely polarized ω , and show that the partial width for the former is a few times larger than for the latter. We work for simplicity in the low-density expansion, which allows us to develop simple and instructive formulas for the amplitude and the decay width in the case when the 3-momentum of the ω meson

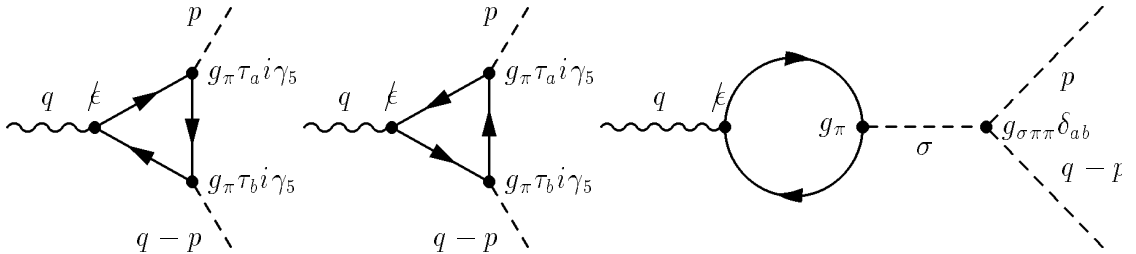


Fig. 2. Same as Fig. 1 evaluated in the linear σ -model. In this case pseudoscalar π - N coupling is used, and the third diagram involves the intermediate σ meson propagator, $1/(m_\sigma^2 - m_\omega^2)$. The π - N and σ - N coupling constants are equal and denoted by g_π . The $g_{\sigma\pi\pi}$ coupling constant is equal to $(m_\sigma^2 - m_\pi^2)/F_\pi$.

is small, and close to the chiral limit.

In hadronic calculations involving pions one has to choose whether to use pseudovector or pseudoscalar πN coupling. In the latter case one has also to include the scalar-isoscalar σ meson. In case of low-energy physical processes, where all external four-momenta are small, the two methods are equivalent and it is a matter of convenience which coupling to use [15–17]. In the present case the four-momentum of the on-shell ω meson is not small, therefore the two methods do not yield the same result. Only in a formal limit of very large σ mass (or, equivalently, low ω mass) do the results overlap. We will discuss this point very carefully throughout this Letter. Our calculation of $\omega \rightarrow \pi\pi$ in nuclear matter includes the mechanism of absorption of the ω meson by a nucleon from the Fermi sea, and emission of two pions by this nucleon. These processes are depicted in Fig. 1 and Fig. 2, respectively, for the case of pseudovector and pseudoscalar πN coupling. The ωN coupling constant can be estimated from the vector dominance model. We use $g_\omega = 10$. The solid line in Figs. 1 and 2 denotes the in-medium nucleon propagator, which can be conveniently decomposed in the free and density parts

$$G(k) \equiv G_F(k) + G_D(k) = (\not{k} + M) \left[\frac{1}{k^2 - M^2 + i\varepsilon} + \frac{i\pi}{E_k} \delta(k_0 - E_k) \theta(k_F - |\vec{k}|) \right]. \quad (1)$$

The first two diagrams in Figs. 1 and 2 involve triangles with nucleon lines. The only non-vanishing contributions involve one G_D propagator and two G_F propagators. The third diagrams involve the bubbles with two nucleon propagators, and are non-zero only when one propagator is G_D , and the other one G_F . The third diagram in Fig. 1 contains the $\pi\pi NN$ vertex, which involves the pion-nucleon σ term, $\sigma_{\pi N} \simeq 45\text{MeV}$. The process included in the third diagram in Fig. 2 involves the intermediate σ -meson propagator, which in the σ -model takes the simple form $1/(q^2 - m_\sigma^2)$.

The amplitude, evaluated according to diagrams in Fig. 1 or Fig. 2 can be decomposed in the following Lorentz-invariant way

$$\mathcal{M} = \epsilon^\mu (A p_\mu + B u_\mu + C q_\mu), \quad (2)$$

where p is the momentum of one of the pions, q is the momentum of the ω meson, u is the four-velocity of nuclear matter, and ϵ specifies the polarization of ω . For the case of the pseudovector coupling (Fig. 1) the explicit calculation (in the rest frame of the nuclear matter) yields:

$$A^{\text{PV}} = g_\omega \frac{g_A^2}{F_\pi^2} \frac{4(m_\omega^2 + 2m_\pi^2) \cos \gamma}{m_\omega^2(m_\omega^2 - 4M^2)} |\vec{q}| \rho_B + \dots, \quad (3)$$

$$B^{\text{PV}} = g_\omega \left[\frac{g_A^2}{F_\pi^2} \frac{2m_\omega^2}{m_\omega^2 - 4M^2} - \frac{\sigma_{\pi N}}{F_\pi^2} \frac{8M}{m_\omega^2 - 4M^2} \right] \rho_B + \dots, \quad (4)$$

$$C^{\text{PV}} = g_\omega \left[-\frac{g_A^2}{F_\pi^2} \frac{2(m_\omega^3 + (m_\omega^2 + 2m_\pi^2) \cos \gamma |\vec{q}|)}{m_\omega^2(m_\omega^2 - 4M^2)} + \frac{\sigma_{\pi N}}{F_\pi^2} \frac{8M}{m_\omega(m_\omega^2 - 4M^2)} \right] \rho_B + \dots. \quad (5)$$

where γ is the angle between \vec{q} and \vec{p} , and ... mean higher-order terms in the baryon density ρ_B , momentum $|\vec{q}|$, and the chiral parameter m_π . We chose to present the results in the lowest expansion in these three parameters due to simplicity. We should also comment here that in fact it is not justified to keep terms in the density expansion which are of order ρ_B^2 or higher, since these result from diagrams not included in the calculation.²

For the case of the pseudoscalar coupling (Fig. 2) we get analogously

$$A^{\text{PS}} = g_\omega \frac{g_\pi^2}{M^2} \frac{4(m_\omega^2 + 2m_\pi^2) \cos \gamma |\vec{q}|}{m_\omega^2(m_\omega^2 - 4M^2)} \rho_B + \dots, \quad (6)$$

$$B^{\text{PS}} = g_\omega \frac{g_\pi^2}{M^2} \left[2 + \frac{8M^2(m_\sigma^2 - m_\pi^2)}{(m_\omega^2 - 4M^2)(m_\sigma^2 - m_\omega^2)} \right] \rho_B + \dots, \quad (7)$$

$$C^{\text{PS}} = g_\omega \frac{g_\pi^2}{M^2} \left[-\frac{2(m_\omega^3 + (m_\omega^2 + 2m_\pi^2) \cos \gamma |\vec{q}| - 4M^2 m_\omega)}{m_\omega^2(m_\omega^2 - 4M^2)} - \frac{8M^2(m_\sigma^2 - m_\pi^2)}{m_\omega(m_\omega^2 - 4M^2)(m_\sigma^2 - m_\omega^2)} \right] \rho_B + \dots. \quad (8)$$

Eqs. (3-5) and Eqs. (6-8) are equivalent if the following conditions are satisfied: (i) the Goldberger-Treiman relation holds, *i.e.* $g_A M = g_\pi F_\pi$, (ii) the pion-nucleon sigma term satisfies the σ -model relation $\sigma_{\pi N} = g_A^2 M m_\pi^2 / m_\sigma^2$, and (iii) $m_\sigma^2 / m_\omega^2 \rightarrow \infty$. Condition (i) follows from chiral symmetry and is satisfied well with experimental numbers. Condition (ii) and (iii) are formal. When imposed, they lead the strong cancellations between the “triangle” and “bubble” diagrams, which can now be explicitly observed in the form of the coefficients B and C in Eqs. (7,8). In realistic cases, however, the third condition is not well satisfied and the cancellations are weaker. In the extreme situation, for m_σ approaching m_ω , the ω decay width strongly increases and the σ diagram dominates. However, in this case the approach should include the finite width of σ , which eliminates the divergence [14].

The expression for the decay width reads [18]

$$\Gamma_{\omega \rightarrow \pi\pi} = \frac{1}{2} 3 \frac{1}{n_s} \sum_s \frac{1}{2q_0} \int \frac{d^3 p}{(2\pi)^3 2p_0} \int \frac{d^3 p'}{(2\pi)^3 2p'_0} |\mathcal{M}|^2 (2\pi)^4 \delta^{(4)}(q - p - p'), \quad (9)$$

where the factor $\frac{1}{2}$ is the symmetry factor when the decay proceed into two neutral pions, the factor of 3 accounts for the isospin degeneracy of the final pion states (*i.e.* neutral and charged pions), n_s is the number of spin states of the ω meson, and \sum_s denotes the sum over these spin states, and q , p and $p' = q - p$ are the four-momenta of the ω meson,

² The next terms in the density expansion are the Fermi-motion correction, which start at $\rho_B^{4/3}$. These could be included, but technically it is rather involved for the triangle diagrams in Figs. 1 or 2. Hopefully, these are not too large, as was the case *e.g.* in model calculations of the density-dependence of the quark condensate [17].

and the two pions, respectively (cf. Figs. 1 and 2). The phase-space integral is performed in the rest frame of the nuclear medium, and we obtain explicitly

$$\Gamma_{\omega \rightarrow \pi\pi} = \frac{1}{2} 3 \frac{1}{n_s} \sum_s \frac{1}{2q_0} \int \sin \gamma \frac{\vec{p}^2}{8\pi p_0 (q_0 - p_0) |a|} |\mathcal{M}|^2 d\gamma, \quad (10)$$

where the kinematics enforces

$$\begin{aligned} |\vec{p}| &= \frac{m_\omega^2 |\vec{q}| \cos \gamma + q_0 \sqrt{m_\omega^4 - 4m_\pi^2 (m_\omega^2 + \vec{q}^2 \sin^2 \gamma)}}{2(m_\omega^2 + \vec{q}^2 \sin^2 \gamma)}, \quad q_0 = \sqrt{m_\rho^2 + \vec{q}^2}, \\ p_0 &= \sqrt{m_\pi^2 + \vec{p}^2}, \quad a = \left. \frac{d(q_0 - \sqrt{m_\pi^2 + r^2} - \sqrt{m_\pi^2 + r^2 - 2r|\vec{q}| \cos \gamma + \vec{q}^2})}{dr} \right|_{r=|\vec{p}|}. \end{aligned} \quad (11)$$

The presence of the medium results in the splitting of transversely and longitudinally polarized ω states. Transversely polarized ω has two helicity states ($n_s = 2$), with projection $s = \pm 1$ on the direction of \vec{q} , and the longitudinally polarized ω has one helicity state ($n_s = 1$), with the corresponding projection $s = 0$. An explicit calculation yields

$$\begin{aligned} \sum_{s=\pm 1} \varepsilon_{(s)}^\mu \varepsilon_{(s)}^\nu &= g^{\mu\nu} - u^\mu u^\nu - \frac{(q^\mu - q \cdot u u^\mu)(q^\nu - q \cdot u u^\nu)}{q \cdot q - (q \cdot u)^2} \equiv T^{\mu\nu}, \\ \varepsilon_{(s=0)}^\mu \varepsilon_{(s=0)}^\nu &= -\frac{q^\mu q^\nu}{q \cdot q} + u^\mu u^\nu + \frac{(q^\mu - q \cdot u u^\mu)(q^\nu - q \cdot u u^\nu)}{q \cdot q - (q \cdot u)^2} \equiv L^{\mu\nu}. \end{aligned} \quad (12)$$

Note that by summing over all polarization we recover $\sum_{s=0,\pm 1} \varepsilon_{(s)}^\mu \varepsilon_{(s)}^\nu = g^{\mu\nu} - \frac{q^\mu q^\nu}{q \cdot q}$. The tensors $T^{\mu\nu}$ and $L^{\mu\nu}$ are projection tensors, *i.e.*, $T^{\mu\nu} T_\nu^\alpha = T^{\mu\alpha}$, $L^{\mu\nu} L_\nu^\alpha = L^{\mu\alpha}$, and $T^{\mu\nu} L_\nu^\alpha = 0$. Furthermore, $T^{\mu\nu} q_\nu = 0$ and $L^{\mu\nu} q_\nu = 0$, which reflects current conservation, as well as $T^{\mu\nu} u_\nu = 0$. Using relations (2,12) in Eq. (10) we find the following expressions for the decay widths of transversely and longitudinally polarized ω meson into two pions:

$$\Gamma_{\omega \rightarrow \pi\pi}^T = A^2 p_\mu T^{\mu\nu} p_\nu, \quad \Gamma_{\omega \rightarrow \pi\pi}^L = (A p_\mu + B u_\mu) L^{\mu\nu} (A p_\nu + B u_\nu). \quad (13)$$

We note that the coefficient C does not enter these formulas. For the case of pseudovector coupling we obtain:

$$\Gamma_{\omega \rightarrow \pi\pi}^{T,PV} = \frac{g_\omega^2}{40\pi} \left(\frac{g_A}{F_\pi} \right)^4 \frac{m_\omega^2 - 2m_\pi^2}{m_\omega(m_\omega^2 - 4M^2)^2} \vec{q}^2 \rho_B^2 + \dots, \quad (14)$$

$$\Gamma_{\omega \rightarrow \pi\pi}^{L,PV} = \frac{g_\omega^2}{5\pi} \left(\frac{g_A}{F_\pi} \right)^4 \frac{m_\omega^2 - 2m_\pi^2 - 10M g_A^{-2} \sigma_{\pi N}}{m_\omega(m_\omega^2 - 4M^2)^2} \vec{q}^2 \rho_B^2 + \dots, \quad (15)$$

where ... denote higher-order terms in the expansion in ρ_B , \vec{q} , and m_π . We note that if the term with $\sigma_{\pi N}$ (which is of the order m_π^2) were neglected, then the width of the

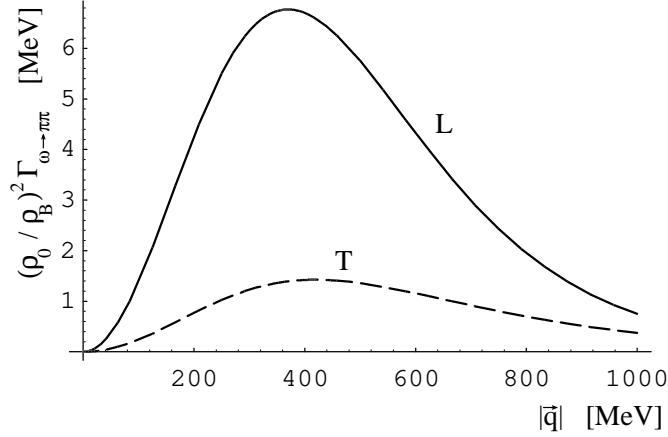


Fig. 3. The quantity $(\rho_0/\rho_B)^2 \Gamma_{\omega \rightarrow \pi\pi}$ plotted as a function of the 3-momentum of the ω meson, $|\vec{q}|$. The solid (dashed) line correspond to the longitudinal (transverse) mode.

longitudinal mode, (15), would be 8 times larger than the width of the transverse mode, (14). However, numerically we find $-10Mg_A^{-2}\sigma_{\pi N}/(m_\omega^2 - 2m_\pi^2) \simeq -0.3$, which is large, and our expansion gives $\Gamma_{\omega \rightarrow \pi\pi}^{L,PV}/\Gamma_{\omega \rightarrow \pi\pi}^{T,PV} \simeq 5$. This indicates that with the physical values of the parameters we are not very close to the chiral limit.

For the case of pseudoscalar coupling we find

$$\Gamma_{\omega \rightarrow \pi\pi}^{T,PS} = \frac{g_\omega^2}{40\pi} \left(\frac{g_\pi}{M} \right)^4 \frac{m_\omega^2 - 2m_\pi^2}{m_\omega(m_\omega^2 - 4M^2)^2} q^2 \rho_B^2 + \dots, \quad (16)$$

$$\Gamma_{\omega \rightarrow \pi\pi}^{L,PS} = \frac{g_\omega^2}{5\pi} \left(\frac{g_\pi}{M} \right)^4 \left\{ \frac{m_\omega^2 - 2m_\pi^2 - 10M^2 m_\pi^2/m_\sigma^2}{m_\omega(m_\omega^2 - 4M^2)^2} + \frac{10M^2[(3M^2 - m_\omega^2 + m_\sigma^2)m_\omega^2 + (m_\omega^4/m_\sigma^2 - 12M^2 + m_\omega^2 - 2m_\sigma^2)m_\pi^2]}{m_\omega(m_\omega^2 - 4M^2)^2(m_\omega^2 - m_\sigma^2)^2} \right\} q^2 \rho_B^2 + \dots. \quad (17)$$

We note that Eqs. (16) and (14) are equal. The expression for the width of the longitudinal mode, Eq. (17), is written in such a way that the first term in the curly brackets reproduces the pseudovector-coupling result, (15), when $\sigma_{\pi N} = g_A^2 M m_\pi^2/m_\sigma^2$. The second term in the curly brackets in (17) comes entirely from the σ -diagram in Fig. 2. Formally, it vanishes when $m_\sigma^2/m_\omega^2 \rightarrow \infty$. It becomes very large when the positions of the σ and ω resonances are close to each other, even when we supply σ with finite width, as in Ref. [14].

In Fig. 3 we present numerical results for the pseudovector-coupling case for *finite* q and m_π , but still in the low-density approximation. We plot the quantities $(\rho_0/\rho_B)^2 \Gamma_{\omega \rightarrow \pi\pi}^{T,PV}$ and $(\rho_0/\rho_B)^2 \Gamma_{\omega \rightarrow \pi\pi}^{L,PV}$, where ρ_0 is the nuclear saturation density, as functions of the momentum $|\vec{q}|$. This way we get rid of the density dependence. Also, in order to obtain more reasonable numerical estimates, we depart in this calculation from the strict low-density limit by reducing the value of the nucleon mass to 70% of its vacuum value, which is a typical in-medium number (*i.e.* $M^*/M = 0.7$). This is a very important effect, since expressions (14-17) scale approximately as M^{-8} . The density dependence on other quantities is less

crucial, so we do not take it into account. The plot shows that the width of the longitudinal mode is a few times larger than the width of the transverse mode for all values of $|\vec{q}|$. We note strong dependence on $|\vec{q}|$, with maxima around 400MeV. The values around the maxima for $\rho_B = 2\rho_0$ give $\Gamma_{\omega \rightarrow \pi\pi}^{T,PV} \simeq 5\text{MeV}$ and $\Gamma_{\omega \rightarrow \pi\pi}^{L,PV} \simeq 25\text{MeV}$. The latter value is substantial, showing that the $\omega \rightarrow \pi\pi$ process should be included (among other processes) in the analysis of the in-medium modification of the ω meson.

In conclusion, we would like to remark on the possibly large role of the final-state interactions. In fact, the σ -diagram of Fig. 2 may be viewed as an example of a process where the pions form a resonance in the final state. This can lead to a large enhancement of the amplitude, as was the case in Ref. [14], and which is explicit in our expressions when m_σ is close to m_ω . However, final-state interactions should be included in all diagrams of Fig. 2 (or Fig. 1), hence cancellations are expected to occur. This interesting extension of the present analysis is left for a future work.

References

- [1] CERES Collab., G. Agakichiev *et al.*, Phys. Rev. Lett. **75** (1995) 1272
- [2] HELIOS/3 Collab., M. Masera *et al.*, Nucl. Phys. **A590** (1995) 3c
- [3] L. S. Celenza, A. Pantziris, and C. M. Shakin, Phys. Rev. **C45** (1992) 205
- [4] H.-C. Jean, J. Piekarewicz, and A. G. Williams, Phys. Rev. **C49** (1994) 1981
- [5] W. Cassing, W. Ehehalt, and C. M. Ko, Phys. Lett. **B363** (1995) 35
- [6] G. Q. Li, C. M. Ko, and G. E. Brown, Nucl. Phys. **A606** (1996) 568
- [7] T. Hatsuda, H. Shiomi, and H. Kuwabara, Prog. Theor. Phys. **95** (1996) 1009
- [8] F. Klingl, N. Kaiser, and W. Weise, Nucl. Phys. **A624** (1997) 527
- [9] B. Friman, talk given at APCTP Workshop on Astro-Hadron Physics: Properties of Hadrons in Matter, Seoul, Korea, 25-31 Oct 1997; GSI-preprint-98-7, nucl-th/9801053 (unpublished)
- [10] V. L. Eletsky, B. L. Ioffe, and J. I. Kapusta, FAU-TP3-98-14, nucl-th/9807072 (unpublished)
- [11] B. Friman, GSI-preprint-98-52, nucl-th/9808071 (unpublished)
- [12] *Hadrons in Nuclear Matter*, edited by H. Feldmaier and W. Nörenberg (GSI, Darmstadt, 1995), proc. Int. Workshop XXIII on Gross Properties of Nuclei and Nuclear Excitations, Hirschegg, Austria, 1995
- [13] *Quark Matter 96*, proc. 12th Int. Conf. on Ultra-Relativistic Nucleus-Nucleus Collisions, Heidelberg, Germany, 1996, Nucl. Phys. **A610**, and references therein
- [14] G. Wolf, B. Friman, and M. Soyeur, GSI-preprint-97-37, nucl-th/9707055 (unpublished)
- [15] S. L. Adler and R. F. Dashen, *Current algebras* (Benjamin, New York, 1968)

- [16] V. D. Alfaro, S. Fubini, G. Furlan, and C. Rossetti, *Currents in hadronic physics* (North Holland, Amsterdam, 1973)
- [17] M. C. Birse, J. Phys. **G20** (1994) 1537
- [18] J. D. Bjorken and S. D. Drell, *Relativistic Quantum Mechanics* (McGraw-Hill, New York, 1965)